CrossMark

Carboxylation kapok fiber as a low-cost, environmentally friendly adsorbent with remarkably enhanced adsorption capacity for cationic dyes

Xiulan Zhang[1] · Chunting Duan[2] · Xin Jia[1] ·
Bin Dai[1]

Abstract   A new surface dicarboxylatic kapok fiber (DC-KF) was prepared by surface modification. During the sorbent preparation, the response surface methodology based on the experimental design of central composite design was employed to select the optimum conditions. Fourier transform infrared, scanning electron microscopy, X-ray diffraction, thermogravimetry, and X-ray photoelectron spectroscopy were employed to investigate the structures of raw, wax removed, and surface DC-KF. As a novel sorbent, it was used in removing cationic dyes of natural red, methylene blue, and rhodamine 6G. The influences of contact time, pH, dye concentration, and ionic strength on dye removal were studied. The adsorption kinetics and isotherms were analyzed. Results showed that the dyes adsorbed onto DC-KF could reach the equilibrium within 1 h. The maximum adsorption capacities calculated from the Langmuir model were 816.4, 524.4, and 613.4 mg/g for NR, MB, and Rh-6G, respectively. The pH and ionic strength had a significant effect on dye removal. Excellent regeneration property demonstrated that DC-KF had the potential of actual applications. For its high adsorption capacity, excellent regeneration, low cost, simple preparation, and complete environmental friendliness, DC-KF will be an excellent candidate for treating cationic dye polluted water.

Keywords   Cationic dye · Kapok fiber · Adsorption

✉ Xin Jia
    jiaxin@shzu.edu.cn

✉ Bin Dai
    db_tea@shzu.edu.cn

1   School of Chemistry and Chemical Engineering/Key Laboratory for Green Processing of Chemical Engineering of Xinjiang Bingtuan, Shihezi University, Shihezi 832003, People's Republic of China

2   Laboratory of Polymer Physics and Chemistry, Institute of Chemistry, Chinese Academy of Sciences, Beijing 100190, People's Republic of China

Introduction

Dyes have brought us a vivid and colorful world. However, hazards lurk when we enjoy this visual banquet. Many dyes are discharged by dyeing, tannery, textile, and paint industries [20, 36]. The discharged dyes in water with strong color will adsorb sunlight and reduce light penetration, which will affect the growth of aquatic organisms and microbes. Also, toxicity, dissolved oxygen consumption, and bio-recalcitrant will lead to huge risks to environmental safety [3, 18]. Involved are three types of dyes: anionic dyes, reactive dyes, and cationic dyes. Among those, cationic dyes are more toxic because of their high tinctorial values and facility of combining with negatively charged phospholipid bilayers of the cell membrane, which will especially impede the growth of plants [7]. Therefore, there are responsibilities and challenges to control and manage cationic dye contamination. At present, many feasible methods, including adsorption [10, 26], ion-exchange [7], biological [24], photodegradation [46], and chemical oxidation [9], have been much investigated for dye removal from wastewater [47]. Among these methods, due to the simple operation, high removal efficiency, low secondary pollution, and abundant raw material source, adsorption is the most attractive method [45, 48]. However, to be an ideal adsorbent, it is obligatory to provide the characterizations of efficiency, economy, and biodegradation. Natural materials always have the properties of economy and biodegradation. However, few of them are efficient. Therefore, modification is necessary for them to serve as ideal adsorbents.

Kapok fiber (KF) is a type of agriculture product that is obtained from the fruits of the silk-cotton tree [39]. It has a distinct hollow-tube structure with a hollow rate of above 86 %, and a wall thickness of about 0.8–1.0 μm [17]. The walls mainly comprise about 64 % cellulose, 13 % lignin, 2.5 % xylan, and 0.8 % wax [32]. Due to the properties of hydrophobic, as an adsorbent, KF is gaining more attention as an alternate for oil removal [5, 40–42], rarely in aqueous solution [12, 56]. Some researches have reported that the cellulose and lignin can remove dyes from aqueous solution [4, 36]. However, for KF, the hydrophobicity and low density make it difficult to disperse in aqueous solutions. Therefore, it is a prerequisite to change the wettability of KF to achieve hydrophilicity so as to be used as a dye adsorbent. Treating with sodium chlorite to remove the surface wax is an effective method for KF to gain hydrophilicity [21]. Additionally, for cationic dye removal, it is better for the adsorbent to contain some functional groups, such as a sulfonic acid group or a carboxyl group, which can possess negative points in aqueous solution. It has been reported that 2,3-dicarboxy cellulose can be easily obtained by treating cellulose with sodium periodate and sodium chlorite [22]. So, based on the high cellulose content of KF, it is available to generate carboxyl groups on the surface of KF by surface modification.

According to the numerous advantages, KF here is employed to prepare a new adsorbent [surface 2,3-dicarboxy cellulose kapok fiber (DC-KF)] for cationic dye removal, which has excellent hydrophilicity, and is fully environmentally friendly. To select the optimum conditions, response surface methodology (RSM), an experimental strategy for seeking the optimum conditions for a multivariable system, is an efficient technique for optimization and is employed [11]. In this work,

Scheme 1 Periodate oxidation of TKF
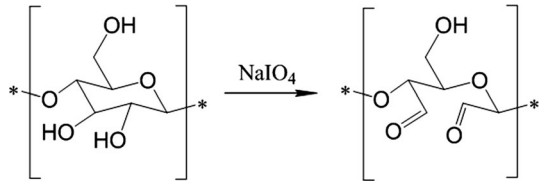
RSM uses the experimental design of central composite design (CCD) to fit the model by least squares technique [1].

Materials and methods

Materials

Kapok fiber with a length of 50–100 μm was supplied by Prof. Jian Xu's group from Sichuan Province. Sodium chlorite, sodium periodate, calcium chloride, and Natural red (NR) were bought from Tianjin Guangfu Fine Chemical Research Institute. Rhodamine 6G (Rh-6G) was obtained from J&K Scientific Limited. Methylene blue (MB) was purchased from Sanxi'an chemical reagent factory. All reagents were used as received, and all aqueous solutions were prepared with distilled water.
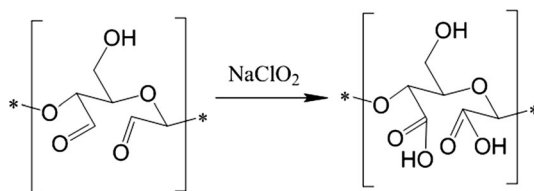
Preparation of DA-KF

Firstly, the KF was treated with sodium chlorite to remove the botanic wax [21]. In detail, 6 g of KF was dispersed in 400 ml of $NaClO_2$ solution and stirred for 1 h at 70 °C. Then the fibers were washed to neutrality with distilled water and dried at 60 °C under vacuum. The treated KF was labeled as TKF. The surface 2,3-dialdehyde cellulose kapok fiber (DA-KF) was prepared by the method of surface in situ oxidation. As follows: with stirring, 0.25 g of TKF was dispersed in 30 ml of distilled water, and 0.2 g $CaCl_2$ was added as a cellulose activator [34]. An appropriate amount of $NaIO_4$ was added while the temperature reached the designed value and was stirred for 3 h in dark and then washed to neutrality with distilled water and filtered. After freeze drying, the DA-KF was obtained. The surface reaction process is shown in Scheme 1.

Preparation of DC-KF

For DC-KF preparation, $NaClO_2$ played the role of mild oxidant. In the process, 0.2 g DA-KF was dispersed in 50 ml of solution with $NaClO_2$ concentration of 0.05 M and the pH value of 5.0 (adjusted by acetic acid). After the mixture was stirred for 24 h, the DC-KF was obtained. The oxidation reaction is shown in Scheme 2.

Scheme 2 Sodium chlorite
oxidation of DA-KF

Central composite design

CCD was employed for the optimization of two variables, which are the amount of NaIO$_4$ and reaction temperature in DA-KF preparation. The prepared DA-KF was further oxidized to DC-KF by a slight excess of NaClO$_2$ with the same amount. In this design model, the reaction temperature (60–80 °C) and the amount of NaIO$_4$ (0.15–0.35 g) were taken as input variables (Table 1), and the adsorption capacities of DC-KF for NR, MB, and Rh-6G were taken as the responses. Response surface was created using Design Expert Software Version 8.0.6 (STAT-EASE Inc., Minneapolis, MN, USA).

Characterization

FTIR spectra were recorded on a Thermo Nicolet NEXUS TM spectrophotometer using KBr pellets in the range of 400–4000 cm^{-1}. The micrographs of samples were observed using SEM (JSM-5600LV, JEOL) after fixing the samples on aluminum stubs and coating with gold. The specific surface area of samples was determined by nitrogen adsorption–desorption isotherms at 77 K using Brunauer–Emmett–Teller method (BET, ASAP2020, Micromeritics Inc.). The XRD patterns were obtained from D8 ADVANCE X-ray diffractometer equipped with a Cu-Kα radiation source. Thermogravimetry (TG, STA449F$_3$) was employed to determine the thermal stability of samples. The thermograms were obtained under a nitrogen atmosphere at a uniform heating rate of 2.5 °C/min from ambient temperature to 600 °C. The X-ray photoelectron spectroscopy (XPS: AMICUS) analysis was carried out by using Al Kα X-ray source (1258.6 eV).

Adsorption and desorption

The adsorption experiments were carried out by mixing 10 mg DC-KF with 50 ml of dye solution in 100-ml Erlenmeyer flasks in a thermostatic shaker with constant shaking at 140 rpm. Among those, 0.1 M NaOH and 0.1 M HCl were employed to

Table 1 Experimental range and levels of independent variables for the process of DA-KF preparation

Factors	Range and levels (coded)			
	−1 level	+1 level	−alpha	+alpha
Reaction temperature (°C)	60	80	55.86	84.14
Amount of NaIO$_4$ (g)	0.15	0.35	0.11	0.39

adjust the pH value. After adsorption, the absorbent was collected by centrifugation, and the concentrations of dyes before and after adsorption were determined through Vis spectrophotometry (V-1100D) at 530, 658, and 523 nm for NR, MB, and Rh-6G, respectively. The adsorption kinetics was firstly conducted at various contact time ranging from 0 to 3 h at 25 °C with initial dye concentration of 200 mg/l at neutral pH. The pH-dependence adsorption was investigated by adjusting the pH from 3.0 to 8.0 for NR, 2.0 to 10.0 for MB, and Rh-6G respectively, with an initial concentration of 200 mg/l, time of 3 h and temperature of 25 °C. The adsorption isotherm study was carried out in different dye initial concentrations ranging from 50 to 300 mg/l, with the time of 3 h, temperature of 25 °C, and pH value of 7.0. To study the effect of ionic strength on dye removal, the sodium chloride (NaCl) was employed to adjust the solution ionic strength ranging from 0 to 0.2 M, keeping the initial concentration of 165 mg/l for NR, 210 mg/l for MB, and 200 mg/l for Rh-6G, time of 3 h, pH of 7.0, and temperature of 25 °C, respectively. HCl (0.1 M), NaOH (0.1 M) and ethyl alcohol were used for desorption, respectively. Desorption efficiency was investigated to select the most efficient desorption reagent.

Results and discussion

Characterizations of samples

The FTIR spectra of KF, TKF, DA-KF and DC-KF are displayed in Fig. 1A. Compared with raw kapok fiber, the NaClO$_2$ treated kapok fiber (TKF) had a
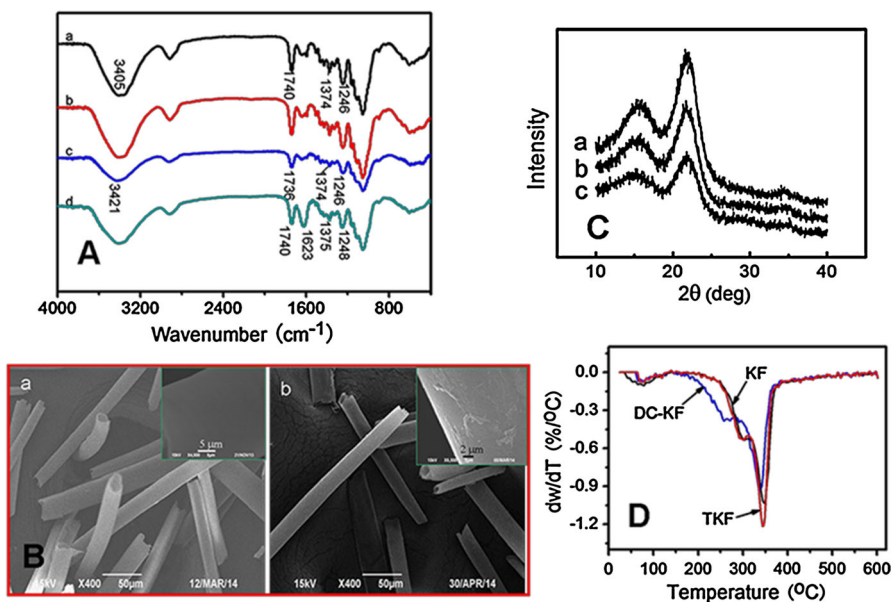

Fig. 1 **A** FTIR spectra of *a* KF, *b* TKF, *c* DA-KF, and *d* DC-KF. **B** SEM images of *a* TKF, *b* DC-KF. **C** XRD pattern of *a* KF, *b* TKF and *c* DC-KF. **D** DTG curves of KF, TKF, and DC-KF

broader and stronger band at 3405 cm^{-1}, which was assigned to O–H stretching vibration mainly from cellulose or lignin, implying the successful removal of plant wax from fiber surface and the increment of cellulose hydroxyl groups [39]. However, the absorption peak belonged to C=O stretching vibration of ketones, carboxylic groups, and esters in lignin and acetyl ester groups in xylan at 1740 cm^{-1} [42] had no obvious change, which indicated that the NaClO$_2$ treatment had no destruction to lignin and xylan. After treating with NaIO$_4$, the band of O–H stretching vibration had a blue shift and moved to 3421 cm^{-1}. This was attributed to that the conjugated structure of cellulose was broken, and some hydroxyl of cellulose on the TKF surface might be oxidized to aldehyde by NaIO$_4$ and the formed 2, 3-dialdehyde cellulose. For DC-KF spectra, there was a new and strong band that appeared at 1623 cm^{-1} corresponding to bending vibration of water. This may be because of the combination of the formed dicarboxylic and water.

SEM images of TKF and DC-KF are shown in Fig. 1B. It was observed that the structures of air-filled lumen kept integrated after being treated with NaClO$_2$ and further oxidation. The surface of TKF was smooth and silky, however, some gullies were observed on a rough surface after two oxidation processes. The results demonstrated that the surface but the structure of fibers had some changes after the NaClO$_2$ treating and further oxidation. Additionally, the measured BET surface of DC-KF was 3.47 m^2/g, while the TKF and KF BET surfaces were only 1.34 and 0.78 m^2/g.

The XRD patterns in Fig. 1C show two major diffraction peaks close to 15.5 and 22.1 corresponding to the (101) and (002) peaks for all the samples. Clearly, the intensity of each peak for samples was decreased in the order of KF, TKF, DC-KF, which indicated varies of crystallinities. According to the method of segal, the crystallinity index CrI was determined follows Eq. (1) [39]:

$$CrI = \frac{I_{002} - I_{am}}{I_{002}} \times 100\%$$ (1)

where I_{002} ($2\theta = 22.1$) includes both amorphous and crystalline material, I_{am} ($2\theta = 18.0$) represents amorphous material only.

It was calculated that the CrI of KF, TKF, and DC-KF was 35.65, 32.74, and 26.02 %, respectively. The result demonstrated that the crystallinities of the samples were decreasing with further treating. Interestingly, the microstructure of fibers is maintained although the CrI decreased from 35.65 to 26.02 % (Fig. 1B).

As DTG curves show in Fig. 1D, the samples of KF, TKF, and DC-KF demonstrated three weight loss stages. Compared with TKF and DC-KF, the first weight loss band at around 75 °C was broader than that of TKF and DC-KF. This was because the raw kapok fibers contained a small amount of wax, which had a complex compound that had a low decomposition temperature. After being treated by NaClO$_2$, the wax on the KF surface was removed and thus resulted in a narrow weight loss band at around 75 °C that represented the vaporization of water in fibers. At about 303 °C, a decompose peak appeared for KF and TKF, respectively. This result was ascribed to the weight loss of hydroxyl in cellulose. However, the second weight loss peak of DC-KF was located at a lower temperature at about

257 °C that corresponded to the decomposition of carboxyl [28] and hydroxyl. Because, after KF was oxidized by $NaIO_4$ and $NaClO_2$, some other carboxyl groups were formed, and the higher surface area of DC-KF also made the hydroxyl easier to degradate [52]. The third weight loss stage for samples contributed to the splitting of carbon–carbon bonds. The main degradation peak was around 349, 344, and 337 °C for KF, TKF, and DC-KF, respectively. This was due to the larger surface area, which contributed to easier decomposition from the fiber surface.

The XPS was employed to determine the variation of chemical composition of samples surface. As shown in Fig. 2a–c, it is obvious that KF, TKF, and DC-KF mainly consisted of carbon and oxygen, which corresponded to the C1 s spectrum (284.6 eV) and O1 s spectrum (532.5 eV). However, for DC-KF, there had a Na1 s spectrum (1072 eV) regardless of C1 s and O1 s spectrum. This might be the Na^+ from $NaClO_2$ or NaClO that replaced the hydrogen in carboxyl acid or hydrogen during the formation of carboxyl groups. After being treated with $NaClO_2$, the O/C of TKF was increased from 27.7 to 31.9 %, which was attributed to the removal of plant wax that mainly consisted of carbon and hydrogen on the KF surface. The O/C was even raised to 66.4 % for DC-KF, which proved that more oxygen was introduced on the fibers' surface by oxidating with $NaIO_4$ and $NaClO_2$. The O1s spectrum was curve-fitted into three component peaks with binding energies of about 531.6 (C=O), 532.5 (C–O–C/C–O⁻), and 533.3 eV (–OH) to survey the distribution of varies oxygenous groups on fibers surface. It was calculated that the content of C=O (mainly attribute to lignin) and –OH had little change in KF and TKF, but their content had increased about 3 % and decreased about 10 % for C=O and –OH in DC-KF, respectively. This indicated that at least 3 % of –OH had oxidated to C=O, and some –OH had formed the –ONa.
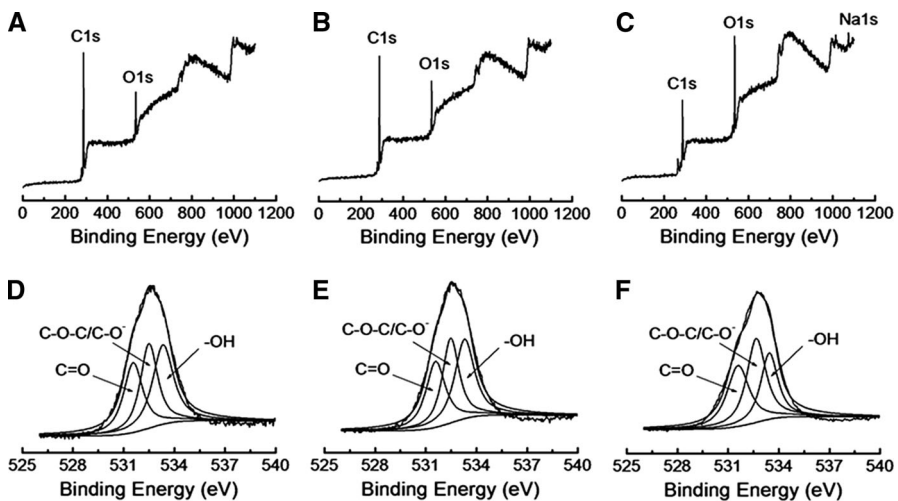

Fig. 2 a–c XPS spectra of KF, TKF, and DC-KF, respectively. d–f XPS analysis of O1 s spectra for KF, TKF, and DC-KF, respectively

RSM optimization

With the adsorption capacity of DC-KF for dye as response, the three-dimensional response surfaces are shown in Fig. 3. It is clear that both the temperature and the amount of $NaIO_4$ in the process of DA-KF preparation had some effect on dye removal. The values of "Prob > F" were 0.0248, 0.001, and 0.0013 for NR, MB, and Rh-6G removal response surface model, respectively. They were all <0.05 indicated all the model terms were significant, whereas, temperature had less of an effect on dye removal compared with $NaIO_4$. This implied that the $NaIO_4$ amount had a bigger contribution than temperature to increase the adsorption capacity of DC-KF. As Fig. 3 shows, the larger $NaIO_4$ amount and a higher temperature were in favor of improving the DC-KF adsorption capacity for MB and Rh-6G. However, they were not the best. Therefore, to obtain an adsorbent that had great adsorption capacity for these three types of dyes, the functions of "numerical optimization" and "point prediction" of CCD-based RSM were used to select the optimum preparation conditions for DA-KF. As a result, when $NaIO_4$ was 0.35 g and temperature was 62.1 °C for DA-KF preparation, DC-KF had the highest predicted adsorption amount of 723.6, 508.6, and 571.8 mg/g, while the experimental actual values were 738.6, 507.5, and 567.2 mg/g, with the relative deviation of 2.07, 0.22, and 0.80 % for NR, MB, and Rh-6G, respectively. According to the result of Wang's group, the $NaClO_2$-treated kapok fiber had the maximum adsorption capacity of 110.13 mg/g for MB [21]. It was found that the surface modification of KF by oxidation enhanced the adsorption capacity for MB.

Effect of contact time and adsorption kinetics

Adsorption kinetics based on contact time is one of the most important parameters to decide the efficiency of an absorbent. Firstly, the effects of contact time on dye removal were investigated as shown in Fig. 4a. The adsorption rate was quite rapid for three dye types and the equilibrium could be reached within 1 h. More importantly, 71.5, 97.4, and 90.3 % of the equilibriums were obtained within 1 min for NR, MB, and Rh-6G, respectively, and 95.9 % of the equilibrium of NR removal was completed within 20 min. This implied that removals of three types of dyes were efficient. Additionally, the results showed that the adsorption capacities of DC-KF for the dyes were NR > Rh-6G > MB. To further study the adsorption process,
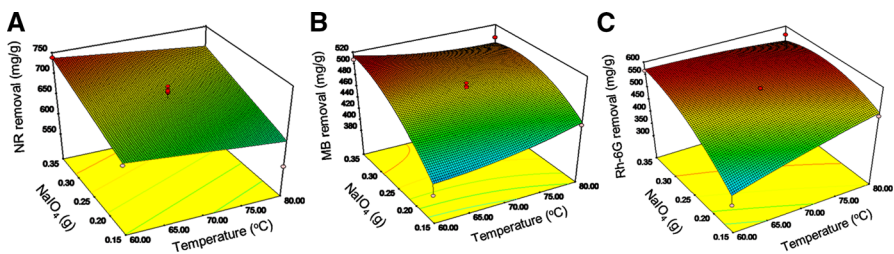

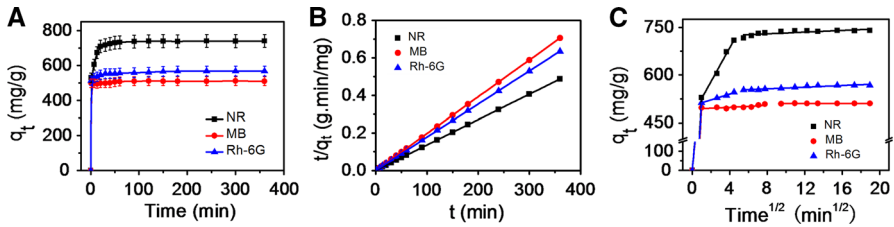**Fig. 3** 3D response surface of adsorption capacity of DC-KF for **a** NR, **b** MB, and **c** Rh-6G

Fig. 4 **a** The effect of contact time ($C_0 = 200$ mg/l, pH $= 7.0$, $T = 25$ °C, $r = 140$ rpm). **b** Plots of pseudo-second-order. **c** Intraparticle diffusion model

the adsorption kinetics were analyzed by fitting for pseudo first-order kinetics [Eq. (2)] [8] and pseudo-second-order kinetics [Eq. (3)] [35] models, respectively.

$$q_t = k_1 q_e e^{(-q_e t)} \qquad (2)$$

$$\frac{t}{q_t} = \frac{1}{k_2 q_e^2} + t\frac{1}{q_e} \qquad (3)$$

where q_t is the amount (mg/g) of dye adsorbed at time t (min), q_e is the adsorption capacity (mg/g) at equilibrium; and k_1, k_1 [g/(mg·min)] are the rates constant for pseudo-first-order and pseudo-second-order models, respectively. The plot of q_t versus t and t/q_t versus t were employed to describe the pseudo-first-order and pseudo-second-order model, respectively. The pseudo-second-order model result is shown in Fig. 4b, and the calculated data are listed in Table 2. The result showed that the adsorption kinetics of the three dyes fit well to the pseudo-second-order model, which assumed that two steps were mainly existed in adsorption process. The first one was fact that adsorbate adsorbed onto the adsorbent could reach equilibrium quickly, and the second was a slower adsorption process, which could continue for a long time [51].

To certify the steps involved in the process of adsorption, the intraparticle diffusion model was analyzed by using the following expression [Eq. (4)] [23]:

$$q_t = k_p t^{1/2} + C \qquad (4)$$

where K_p is the diffusion coefficient, and C is a constant.

Table 2 The determined parameters of pseudo-first-order and pseudo-second-order models

Dyes	Pseudo-first-order		Pseudo-second-order		K_p [mg/(g min$^{1/2}$)]		
	k_1 (g/mg min)	R^2	k_2 (g/mg min)	R^2	K_{p1}	K_{p2}	K_{p3}
NR	1.3306	0.9647	0.00295	0.99997	528.98	53.15	1.34
MB	4.1551	0.9979	0.00864	0.99999	497.37	1.49	0.03
Rh-6G	2.5665	0.9931	0.00266	0.99998	513.03	9.15	1.31

The plot of q_t versus $t^{1/2}$ gives a straight line, in which K_p is the slope and C is the intercept (Fig. 4c). It was obvious that the dyes adsorbed onto DC-KF contented three steps. The related diffusion coefficients of these three steps for dyes transferring to DA-KF were expressed by K_{p1}, K_{p2}, and K_{p3}, respectively, and the values are calculated in Table 3. A higher diffusion coefficient meant a higher adsorption rate, which indicated that the first step had the highest adsorption rate. The second step was following by, and the third step had the lowest adsorption rate. The result was explained as the first step was an instantaneous diffusion stage. During the time, the concentrations of dyes were so high that a large amount of dyes were rapidly adsorbed on the exterior surface of the DC-KF until all of the adsorption sites of the exterior surface were occupied. Then, the second adsorption step occurred. Because of the increased resistance, the adsorption rate was decreased, which was described as dyes entered into the pores of the DC-KF and were adsorbed on the interior surface of the ducts. Finally, with the saturation of adsorption sites of DC-KF and the decrease of dyes concentrations, the intraparticle diffusion rate gradually slowed down and finally reached equilibrium [49].

## Effect of initial dye concentration and adsorption isotherm

The effect of initial concentration on dye adsorption onto DA-KF was investigated in the range of 50–300 mg/l under neutral and 25 °C for 3 h. As shown in Fig. 5a, due to the abundant adsorption sites, the dye in aqueous solution was mostly adsorbed onto DC-KF at the dye concentration of 50 mg/l. The results demonstrated that the adsorption capacity was linearly increased with an increase of the initial dye concentration when the dye concentration was lower than 150 mg/l. It could reach the maximum adsorption capacities of 786.6, 513.7, and 630.0 mg/g for NR, MB, and Rh-6G, respectively. To further study the adsorption properties, two models, the Langmuir isotherm [Eq. (5)] and the Freundlich isotherm [Eq. (6)], were used to analyze the data [6, 54].

$$q_e = \frac{abC_e}{1 + bC_e} \tag{5}$$

Table 3 Langmuir and Freundlich isotherm parameters for dye adsorption on DC-KF

| Dyes	Langmuir			Freundlich		
	b (L/mg)	a (mg/g)	R^2	K_F (mg^{1-n} L^n/g)	n	R^2
NR	0.5907	816.3	0.9557	416.3	6.879	0.7341
MB	0.1908	524.4	0.9938	345.4	13.228	0.9873
Rh-6G	1.4260	613.4	0.9677	355.8	8.215	0.8882
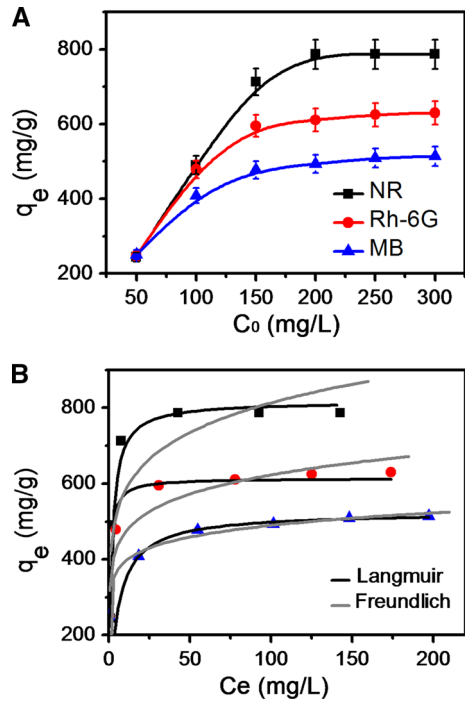
$$q_e = K_F(C_e)^{1/n} \tag{6}$$

where q_e and C_e are the amount of dye adsorbed per unit weight of the adsorbent (mg/g) and the equilibrium concentration of dye (mg/l), respectively; a is the maximum adsorption capacity (mg/g) for fitting; a is a constant related to the free energy of adsorption (L/mg), and K_F and n are the constants for Freundlich model. The isotherm parameters were determined by curve fitting (Fig. 5b) and are shown in Table 3. By comparing the correlation coefficient (R^2) value of the two models, it was not difficult to find that three type dyes adsorbed onto DC-KF were fitted well to Langmuir isotherm, which demonstrated that the adsorbate had equal affinity for the whole adsorption sites [15]. Additionally, the maximum adsorption capacities, which were obtained from Langmuir isotherm, were 816.4, 524.4, and 613.4 mg/g for NR, MB, and Rh-6G, respectively, are higher than many previous adsorbents (Table 4). This result corresponds to the values of the experimental results.

Effect of pH and ionic strength

The pH is an important factor in deciding the sensitivity and surface charge of the adsorbent, and ionization degree of dye [30]. As shown in Fig. 6a, the result displayed the pHs had a significant effect on dye adsorption. The adsorption capacities of DC-KF for dyes were obviously raised with higher pH when the pH was lower than 7.0 for NR, 5.0 for MB, and Rh-6G. This was attributed to the strong

Table 4 Comparison of NR, MB, and Rh-6G maximum adsorption capacities onto other adsorbent

Adsorbent	Dye	Adsorption capacity (mg/g)	References
Pleurotus ostreatus nanoparticles	NR	61.7	Lei et al. [19]
Fe_3O_4 hollow nanospheres	NR	105	Iram et al. [16]
$Zn_3[Co(CN)_6]_2 \cdot nH_2O$ nanospheres	NR	285.7	Wang et al. [41–43]
Cottonseed hull	NR	176.9	Zhou et al. [57]
Polyacrylamide microspheres	NR	1937	Yao et al. [50]
	MB	1977	
	Gentian violet	1850	
Si/Mg modified palygorskite	MB	527.2	Wang et al. [44]
Strychnos potatorum seeds	MB	78.8	Senthamarai et al. [31]
Activated carbon	MB	185	Ghaedi et al. [14]
SBA-15	MB	280	Dong et al. [13]
Goethite nanoadsorbents	MB	9.6	Nassar and Ringsred [25]
Acrylic acid-based superabsorbents	MB	86	Shukla and Madras [33]
	Rh-6G	73	
Chitosan-g-(*N*-vinyl pyrrolidone)/montmorillonite	Rh-6G	36.6	Vanamudan et al. [37]
Urban food waste	Rh-6G	71.4	Parshetti et al. [27]
Chitosan clay nanocomposite	Rh-6G	440.9	Vanamudan and Pamidimukkala [38]
Nanoclay		428.9	
Chitosan		411.3	
Trichoderma harzianummycelial waste	Rh-6G	1.99	Albuquerque et al. [2]
Carboxylation kapok fiber	NR	816.4	This work
	MB	524.4	
	Rh-6G	613.4	
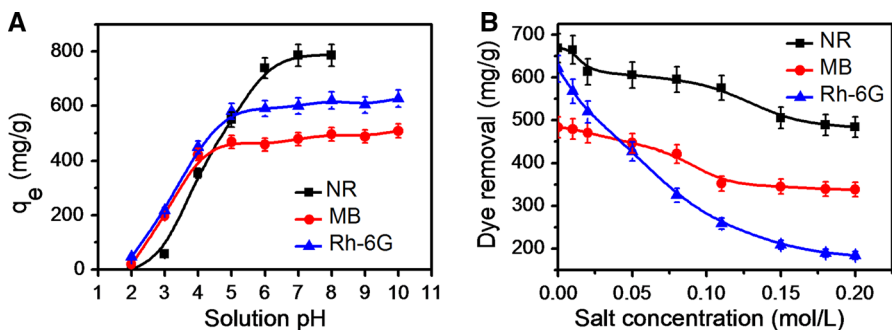
Fig. 6 Effect of **a** pH and **b** ionic strength on dye removal

competition of H^+ combined with $-COO^-$ on DC-KF surface and occupied the adsorption sites at lower pH [29]. At higher pH, the deprotonation of carboxyl was increased, which caused an increase in electrostatic attraction and higher adsorption capacities for cationic dyes [34]. However, adsorption capacities were rarely increased at pH 7.0–8.0 for NR, and 5.0–10.0 for MB and Rh-6G. This is because the available –COOH on adsorbent surface was mostly forming the $-COO^-$, and combining with cationic dyes at pH 5.0. Subsequently, the deprotonation of hydroxyl groups were anabatic increased that increased the adsorption capacity of DC-KF for NR, but they had little contribution to improving the amount of MB and Rh-6G adsorbed onto DC-KF due to their high electronegativities.

Actually, there exist different ionic strengths in different printing and dyeing wastewater, and it may have some effect on dye removal. Therefore, in this study, NaCl was employed to investigate the impact of ionic strength on dye removal. From Fig. 6b, it was found that the ionic strength had a significant effect on dye removal. In detail, for NR and MB removal, the adsorption capacities were obviously decreased with increasing ionic strength when the concentration of NaCl was lower than 0.18 mol/l. Then, they remained unchanged with any further increase in ionic strength. Compared with the original conditions, which were without NaCl, there were 27.7 and 30.1 % of the adsorption capacities for NR and MB reduced. However, for Rh-6G removal, it seemed that the ionic strength had an especially significant effect on Rh-6G that 0.01 mol/l NaCl could result in 8.6 % of the DC-KF adsorption capacity loss, and about 70.4 % of the adsorption capacity for Rh-6G without NaCl was reduced when the concentration of NaCl was 0.2 mol/l. These results might contributed to the Na^+ competing with cationic dye for surface adsorption sites, and also NaCl in solution produced an electrostatic shield between the charges on DC-KF surface [53, 54].

Regeneration

Regeneration property is very important in actual industrial applications. At the same time, a proper selection of desorbent will get a better regeneration property. Therefore, as desorption reagent, ethanol, 0.1 M NaOH, and 0.1 M HCl were studied for regeneration at different times (0.5, 1, 2, and 3 h) to select the best one.

Fig. 7 Regeneration of DC-KF for dye removal
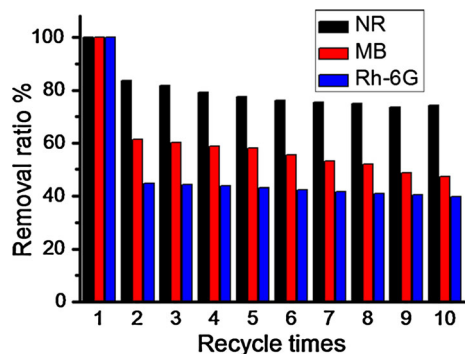
The result gave us the information that DC-KF had a maximum desorption ration in 0.1 M HCl solution, and the desorption time had little effect on it that DC-KF had almost identical desorption ration at 0.5 and 3 h. For adsorption–desorption–adsorption experimental, as shown in Fig. 7, we assumed that the removal ration for first cycle was 100 % for the three dyes. The results demonstrated that the adsorption capacities of DC-KF for the three dyes were suddenly decreased in the second cycle, which was because of the dedoping effect during the desorption process [55]. Then, the removal ratio of DC-KF for the three dyes showed a slow and consecutive decrease. After ten recyclings, the DC-KF still had 74.2, 47.3, and 39.8 % of removal ration for NR, MB, and Rh-6G, respectively. This indicated that DC-KF had a good regeneration property. Summarized, the results of regeneration experiments implied that DC-KF had the potential to remove cationic dyes from aqueous solution in actual applications.

Mechanisms

The dye removal by DC-KF had two mechanisms: physical adsorption and ion exchange. In the process of surface modified of kapok fiber. Some -OH on the surface had oxidated to –COOH or –COONa or formed the –ONa that provide many electric sites. The cationic dyes, such as NR, MB, and Rh-6G, provide positive sites that can easily react with them through ion exchange in aqueous solution. After surface modification, the BET surface and O/C of DC-KF had increased, the hydrophily had improved, and the crystallinity had decreased. Those provide DC-KF with more adsorb sites and contact area for cationic dyes. The physical adsorption and ion exchange are conducted simultaneously. They also can be concluded to adsorption process, and the process of dyes adsorbed on DC-KF is mainly dependent on Langmuir adsorption and pseudo-second-order kinetics.

Conclusions

In conclusion, as a novel sorbent, DC-KF could easily be prepared. Thought the central composite design and response surface methodology, the optimum conditions for DA-KF preparation were the amount of $NaIO_4$ was 0.35 g per 0.25 g TKF and the reaction temperature was 62.1 °C, under which the prepared DC-KF response the adsorption capacities were 738.6, 507.5, and 567.2 mg/g for NR, MB, and Rh-6G, respectively. The dyes adsorbed onto DC-KF were so rapid that the equilibrium could be obtained within 1 h, and the adsorption kinetics fit well to pseudo-second-order. The adsorption capacities of DC-KF for the three types of dyes were increased with increasing solution pH. The maximum adsorption capacities, which were obtained from the Langmuir isotherm model, were 816.4, 524.4, and 613.4 mg/g for NR, MB, and Rh-6G, respectively. The ionic strength had a significant effect on dye removal so that 27.7, 30.1, and 70.4 % of the adsorption capacities were reduced when the concentration of NaCl was 0.2 mol/l for NR, MB, and Rh-6G, respectively. After 10 times recycle, DC-KF still remained high adsorption capacities for dyes. On the whole, the high adsorption capacity, low cost,

being fully environmentally friendly, and excellent regeneration property make DC-KF have an infinite potential in treating cationic dyeing wastewater.

References

1. M. Ahmadi, F. Vahabzadeh, B. Bonakdarpour, E. Mofarrah, M. Mehranian, Application of the central composite design and response surface methodology to the advanced treatment of olive oil processing wastewater using Fenton's peroxidation. J. Hazard. Mater. **123**, 187–195 (2005)
2. R. Albuquerque, M.C. Neves, M.H. Mendonça, T. Trindade, O.C. Monteiro, Adsorption and catalytic properties of SiO_2/Bi_2S_3 nanocomposites on the methylene blue photodecolorization process. Colloids Surf. A **328**, 107–113 (2008)
3. Y. Al-Degs, M. El-Barghouthi, A. El-Sheikh, G. Walker, Effect of solution pH, ionic strength, and temperature on adsorption behavior of reactive dyes on activated carbon. Dyes Pigments **77**, 16–23 (2008)
4. M.A. Al-Ghouti, J. Li, Y. Salamh, N. Al-Laqtah, G. Walker, M.N. Ahmad, Adsorption mechanisms of removing heavy metals and dyes from aqueous solution using date pits solid adsorbent. J. Hazard. Mater. **176**, 510–520 (2010)
5. N. Ali, M. El-Harbawi, A.A. Jabal, C.Y. Yin, Characteristics and oil sorption effectiveness of kapok fibre, sugarcane bagasse and rice husks: oil removal suitability matrix. Environ. Sci. Technol. **33**, 481–486 (2012)
6. T. Basu, K. Gupta, U.C. Ghosh, Performances of As(V) adsorption of calcined (250°C) synthetic iron(III)-aluminum(III) mixed oxide in the presence of some groundwater occurring ions. Chem. Eng. J. **183**, 303–314 (2012)
7. G. Bayramoglu, B. Altintas, M.Y. Arica, Adsorption kinetics and thermodynamic parameters of cationic dyes from aqueous solutions by using a new strong cation-exchange resin. Chem. Eng. J. **152**, 339–346 (2009)
8. D. Bozic, V. Stankovic, M. Gorgievski, G. Bogdanovic, R. Kovacevic, Adsorption of heavy metal ions by sawdust of deciduous trees. J. Hazard. Mater. **171**, 684–692 (2009)
9. C. Chen, P. Gunawan, R. Xu, Self-assembled Fe_3O_4-layered double hydroxide colloidal nanohybrids with excellent performance for treatment of organic dyes in water. J. Mater. Chem. **21**, 1218–1225 (2011)
10. R. Cheng, B. Xiang, Y. Li, Application of nickel(II) complex of dithiocarbamate-modified starch for anionic dyes removal from aqueous solutions. J. Appl. Polym. Sci. **123**, 2439–2444 (2012)
11. I.H. Cho, K.D. Zoh, Photocatalytic degradation of azo dye (Reactive Red 120) in TiO_2/UV system: optimization and modeling using a response surface methodology (RSM) based on the central composite design. Dyes Pigments **75**, 533–543 (2007)
12. C. Duan, N. Zhao, X. Yu, X. Zhang, J. Xu, Chemically modified kapok fiber for fast adsorption of Pb^{2+}, Cd^{2+}, Cu^{2+} from aqueous solution. Cellulose **20**, 849–860 (2013)
13. Y. Dong, B. Lu, S. Zang, J. Zhao, X. Wang, Q. Cai, Removal of methylene blue from coloured effluents by adsorption onto SBA-15. J. Chem. Technol. Biotechnol. **86**, 616–619 (2011)
14. M. Ghaedi, A.M. Ghaedi, F. Abdi, M. Roosta, A. Vafaei, A. Asghari, Principal component analysis-adaptive neuro-fuzzy inference system modeling and genetic algorithm optimization of adsorption of methylene blue by activated carbon derived from *Pistacia khinjuk*. Ecotox. Environ. Saf. **96**, 110–117 (2013)
15. J. Gong, T. Liu, X. Wang, X. Hu, L. Zhang, Efficient removal of heavy metal ions from aqueous systems with the assembly of anisotropic layered double hydroxide nanocrystals@ carbon nanosphere. Environ. Sci. Technol. **45**, 6181–6187 (2011)
16. M. Iram, C. Guo, Y. Guan, A. Ishfaq, H. Liu, Adsorption and magnetic removal of neutral red dye from aqueous solution using Fe_3O_4 hollow nanospheres. J. Hazard. Mater. **181**, 1039–1050 (2010)

17. P.H. Kang, P.J. Jeun, B.Y. Chung, J.S. Kim, Y.C. Nho, Preparation and characterization of glycidyl methacrylate (GNU) grafted kapok fiber by using radiation induced-grafting technique. J. Ind. Eng. Chem. **13**, 956–958 (2007)

18. H. Kyung, J. Lee, W. Choi, Simultaneous and synergistic conversion of dyes and heavy metal ions in aqueous TiO_2 suspensions under visible-light illumination. Environ. Sci. Technol. **39**, 2376–2382 (2005)

19. D.Y. Lei, B. Li, Q. Wang, B. Wu, L. Ma, H. Xu, Removal of neutral red from aqueous solution using *Pleurotus ostreatus* nanoparticles by response surface methodology. Desalin. Water Treat. **54**, 2794–2805 (2014)

20. Q. Li, Q.Y. Yue, H.J. Sun, Y. Su, B.Y. Gao, A comparative study on the properties, mechanisms and process designs for the adsorption of non-ionic or anionic dyes onto cationic-polymer/bentonite. J. Environ. Manage. **91**, 1601–1611 (2010)

21. Y. Liu, J. Wang, Y. Zheng, A. Wang, Adsorption of methylene blue by kapok fiber treated by sodium chlorite optimized with response surface methodology. Chem. Eng. J. **184**, 248–255 (2012)

22. E. Maekawa, T. Koshijima, Properties of 2,3-dicarboxy cellulose combined with various metallic ions. J. Appl. Polym. Sci. **29**, 2289–2297 (1984)

23. M. Min, L. Shen, G. Hong, M. Zhu, Y. Zhang, X. Wang, Y. Chen, B.S. Hsiao, Micro-nano structure poly(ether sulfones)/poly(ethyleneimine) nanofibrous affinity membranes for adsorption of anionic dyes and heavy metal ions in aqueous solution. Chem. Eng. J. **197**, 88–100 (2012)

24. K. Muda, A. Aris, M.R. Salim, Z. Ibrahim, M.C. van Loosdrecht, A. Ahmad, M.Z. Nawahwi, The effect of hydraulic retention time on granular sludge biomass in treating textile wastewater. Water Res. **45**, 4711–4721 (2011)

25. N.N. Nassar, A. Ringsred, Rapid adsorption of methylene blue from aqueous solutions by goethite nanoadsorbents. Environ. Eng. Sci. **29**, 790–797 (2012)

26. F.A. Ozdemir, B. Demirata, R. Apak, Adsorptive removal of methylene blue from simulated dyeing wastewater with melamine-formaldehyde-urea resin. J. Appl. Polym. Sci. **112**, 3442–3448 (2009)

27. G.K. Parshetti, S. Chowdhury, R. Balasubramanian, Hydrothermal conversion of urban food waste to chars for removal of textile dyes from contaminated waters. Bioresour. Technol. **161**, 310–319 (2014)

28. H.D. Pham, V.H. Pham, E.S. Oh, J.S. Chung, S. Kim, Synthesis of polypyrrole-reduced graphene oxide composites by in situ photopolymerization and its application as a supercapacitor electrode. Chem. Eng. J. **29**, 125–129 (2011)

29. Y. Qi, X. Jin, C. Yu, Y. Wang, L. Yang, Y. Li, A novel chelating resin containing high levels of sulfamine group: preparation and its adsorption characteristics towards p-toluenesulfonic acid and Hg(II). Chem. Eng. J. **233**, 315–322 (2013)

30. K.Z. Setshedi, M. Bhaumik, S. Songwane, M.S. Onyango, A. Maity, Exfoliated polypyrrole-organically modified montmorillonite clay nanocomposite as a potential adsorbent for Cr(VI) removal. Chem. Eng. J. **222**, 186–197 (2013)

31. C. Senthamarai, P.S. Kumar, M. Priyadharshini, P. Vijayalakshmi, V.V. Kumar, P. Baskaralingam, K.V. Thiruvengadaravi, S. Sivanesan, Adsorption behavior of methylene blue dye onto surface modified *Strychnos potatorum* seeds. Environ. Prog. Sustain. **32**, 624–632 (2013)

32. M. Shi, H. Xiao, W. Yu, The fine structure of the kapok fiber. Text. Res. J. **80**, 159–165 (2009)

33. N.B. Shukla, G. Madras, Kinetics of adsorption of methylene blue and rhodamine 6G on acrylic acid-based superabsorbents. J. Appl. Polym. Sci. **126**, 463–472 (2012)

34. J. Sirvio, U. Hyvakko, H. Liimatainen, J. Niinimaki, O. Hormi, Periodate oxidation of cellulose at elevated temperatures using metal salts as cellulose activators. Carbohyd. Polym. **83**, 1293–1297 (2011)

35. C. Sun, C. Li, C. Wang, R. Qu, Y. Niu, H. Geng, Comparison studies of adsorption properties for Hg(II) and Au(III) on polystyrene-supported bis-8-oxyquinoline-terminated open-chain crown ether. Chem. Eng. J. **200–202**, 291–299 (2012)

36. D. Suteu, T. Malutan, D. Bilba, Removal of reactive dye brilliant red HE-3B from aqueous solutions by industrial lignin: equilibrium and kinetics modeling. Desalination **255**, 84–90 (2010)

37. A. Vanamudan, K. Bandwala, P. Pamidimukkala, Adsorption property of rhodamine 6G onto chitosan-g-(N-vinyl pyrrolidone)/montmorillonite composite. Int. J. Biol. Macromol. **69**, 506–513 (2014)

38. A. Vanamudan, P. Pamidimukkala, Chitosan, nanoclay and chitosan–nanoclay composite as adsorbents for rhodamine-6G and the resulting optical properties. Int. J. Biol. Macromol. **74**, 127–135 (2015)

39. J. Wang, Y. Zheng, A. Wang, Effect of kapok fiber treated with various solvents on oil absorbency. Ind. Crops Prod. **40**, 178–184 (2012)

40. J. Wang, Y. Zheng, A. Wang, Superhydrophobic kapok fiber oil-absorbent: preparation and high oil absorbency. Chem. Eng. J. **213**, 1–7 (2012)

41. J. Wang, Y. Zheng, A. Wang, Coated kapok fiber for removal of spilled oil. Mar. Pollut. Bull. **69**, 91–96 (2013)

42. J. Wang, Y. Zheng, A. Wang, Investigation of acetylated kapok fibers on the sorption of oil in water. J. Environ. Sci. **25**, 246–253 (2013)

43. W. Wang, C. Li, J. Yao, B. Zhang, Y. Zhang, J. Liuds, Rapid adsorption of neutral red from aqueous solutions by $Zn_3[Co(CN)_6]_2 \cdot nH_2O$ nanospheres. J. Mol. Liquid **184**, 10–16 (2013)

44. W. Wang, G. Tian, Z. Zhang, A. Wang, A simple hydrothermal approach to modify palygorskite for high-efficient adsorption of methylene blue and Cu(II) ions. Chem. Eng. J. **265**, 228–238 (2015)

45. Y. Wang, H. Yang, M. Pschenitza, R. Niessner, Y. Li, D. Knopp, A. Deng, Highly sensitive and specific determination of mercury(II) ion in water, food and cosmetic samples with an ELISA based on a novel monoclonal antibody. Anal. Bioanal. Chem. **403**, 2519–2528 (2012)

46. K. Woan, G. Pyrgiotakis, W. Sigmund, Photocatalytic carbon-nanotube-TiO_2 composites. Adv. Mater. **21**, 2233–2239 (2009)

47. X. Wu, D. Wu, R. Fu, W. Zeng, Preparation of carbon aerogels with different pore structures and their fixed bed adsorption properties for dye removal. Dyes Pigments **95**, 689–694 (2012)

48. H. Xu, Y. Zhang, Q. Jiang, N. Reddy, Y. Yang, Biodegradable hollow zein nanoparticles for removal of reactive dyes from wastewater. J. Environ. Manage. **125**, 33–40 (2013)

49. W. Yang, P. Ding, L. Zhou, J. Yu, X. Chen, F.L. Jiao, Preparation of diamine modified mesoporous silica on multi-walled carbon nanotubes for the adsorption of heavy metals in aqueous solution. Appl. Surf. Sci. **282**, 38–45 (2013)

50. T. Yao, S. Guo, C. Zeng, C. Wang, L. Zhang, Investigation on efficient adsorption of cationic dyes on porous magnetic polyacrylamide microspheres. J. Hazard. Mater. **292**, 90–97 (2015)

51. M. Zhang, Adsorption study of Pb(II), Cu(II) and Zn(II) from simulated acid mine drainage using dairy manure compost. Chem. Eng. J. **172**, 361–368 (2011)

52. W. Zhang, Y. Zhang, C. Lu, Y. Deng, Aerogels from crosslinked cellulose nano/micro-fibrils and their fast shape recovery property in water. J. Mater. Chem. **22**, 11642–11650 (2012)

53. Z. Zhang, Y. Liu, X. Cao, P. Liang, Sorption study of uranium on carbon spheres hydrothermal synthesized with glucose from aqueous solution. J. Radioanal. Nucl. Chem. **295**, 1775–1782 (2012)

54. X. Zhang, X. Jia, G. Zhang, J. Hu, W. Sheng, Z. Ma, J. Lu, Z. Liu, Efficient removal and highly selective adsorption of Hg^{2+} by polydopamine nanospheres with total recycle capacity. Appl. Surf. Sci. **314**, 166–173 (2014)

55. Y. Zheng, Y. Liu, A. Wang, Kapok fiber oriented polyaniline for removal of sulfonated dyes. Ind. Eng. Chem. Res. **51**, 10079–10087 (2012)

56. Y. Zheng, W. Wang, D. Huang, A. Wang, Kapok fiber oriented-polyaniline nanofibers for efficient Cr(VI) removal. Chem. Eng. J. **191**, 154–161 (2012)

57. Q. Zhou, W. Gong, C. Xie, D. Yang, X. Ling, X. Yuan, S. Chen, X. Liu, Removal of neutral red from aqueous solution by adsorption on spent cottonseed hull substrate. J. Hazard. Mater. **185**, 502–506 (2011)